Molecular Therapy
Nucleic Acids
Original Article

Silencing lncRNA LOC101928963 Inhibits Proliferation and Promotes Apoptosis in Spinal Cord Glioma Cells by Binding to PMAIP1

Ying-Juan Zheng,[1,2] Tian-Song Liang,[1,2] Juan Wang,[1] Jing-Yi Zhao,[1] Dao-Ke Yang,[1] and Zhang-Suo Liu[1]

[1]Department of Radiotherapy, The Tumor Hospital of the First Affiliated Hospital of Zhengzhou University, Zhengzhou 475000, P.R. China

Long non-coding RNAs (lncRNAs) have been widely highlighted due to their involvement in various types of cancers, including glioma; however, the exact mechanism and function by which they operate in regard to spinal cord glioma remain poorly understood. LOC101928963 was screened out for its differential expression in spinal cord glioma by microarray analysis. Therefore, this study was conducted to investigate the modulatory effects of LOC101928963 on spinal cord glioma by binding to phorbol-12-myristate-13-acetate-induced protein 1 (PMAIP1). The expression of LOC101928963 and LOC101928963 was characterized in spinal cord glioma tissues, and their interaction was examined by dual-luciferase reporter gene assay. Cells with LOC101928963 that exhibited elevated or suppressed levels of PMAIP1 were established to substantiate the mechanism between LOC101928963 and PMAIP1. qRT-PCR and western blot methods were subsequently applied to determine the expression of cell-proliferation- and apoptosis-related genes in response to the alterations of LOC101928963 and PMAIP1. Glioma cell proliferation and apoptosis were assessed by MTT assay and flow cytometry. Decreased cell apoptosis and PMAIP1 expression, as well as overexpressed LOC101928963, were exhibited among spinal cord glioma tissues. LOC101928963 overexpression was observed to promote cell proliferation and cell-cycle entry and inhibit the process of apoptosis. PMAIP1, a target of LOC101928963, displayed a downregulated level following the elevation of LOC101928963. The present results strongly emphasize the neutralization effect of PMAIP1 overexpression on spinal cord glioma progression induced by the overexpression of LOC101928963. The data obtained during the study highlighted the inhibitory role of LOC101928963 silencing in spinal cord glioma through the increase in PMAIP1, which suggests a potential target in the treatment of spinal cord glioma.

INTRODUCTION

Spinal cord glioma is a rare malignancy, accounting for approximately 20%–25% of all primary spinal cord tumors, with an incidence of approximately 0.22 per 100,000 individuals every year.[1,2] There are four classes of spinal cord tumors, including extradural tumors arising from outside the dura mater, intradural or extraparenchymal tumors located between the dura mater and the spinal cord, and intraparenchymal tumors located in the spinal cord parenchyma.[3] Spinal glioma represents a subtype of intraparenchymal tumors.[4] The low-grade subtype is the most frequently observed subtype, which accounts for 30% to 50% of cases.[5] The forms of spinal cord glioma are often observed in cases of ependymomas and astrocytomas.[6] To date, three main treatment approaches exist for patients suffering from the condition, including resection methods, radiotherapy, and a combination of the two approaches. Spinal glioma remains a complex condition that presents medical health care providers with many difficulties in managing the disease, which is, at times, accompanied by destructive consequences, partially due to the underreporting of clinical data.[2] Therefore, an urgent need exists for elucidation in regard to the understanding of the finer underlying molecular pathogenesis of spinal cord glioma, in a bid to a novel therapeutic strategy for the disease.

In recent years, long non-coding RNAs (lncRNAs), a type of non-coding RNA with a length of more than 200 nt, have been shown to play a role in several crucial biological processes, including tumorigenesis, imprinting control, and cell differentiation.[7] Chiefly, lncRNAs have been indicated to play a crucial role in various cancers, such as glioma, hepatocellular carcinoma, and gastric cancer.[8] A previous study highlighted the differential lncRNA expression between glioma and normal brain tissues.[9] Moreover, lncRNAs could regulate cancer progression through the mediation of cancer-related mRNAs. For example, HOTAIR has been reported to exert its carcinogenesis effort through interaction with the cell-cycle-related mRNA network in glioma.[10] Phorbol-12-myristate-13-acetate-induced protein 1 (PMAIP1), a Bcl-2 homology domain 3 (BH3)-only protein, is a p53-inducible gene that responds to DNA damage.[11] PMAIP1

Received 22 February 2019; accepted 24 July 2019;
https://doi.org/10.1016/j.omtn.2019.07.026.

[2]These authors contributed equally to this work.

Correspondence: Dao-Ke Yang, Department of Radiotherapy, The Tumor Hospital of the First Affiliated Hospital of Zhengzhou University, Zhengdong Branch, Zhengzhou 475000, Henan Province, P.R. China.
E-mail: 15903650068@163.com
Correspondence: Zhang-Suo Liu, Department of Radiotherapy, The Tumor Hospital of the First Affiliated Hospital of Zhengzhou University, Zhengdong Branch, Zhengzhou 475000, Henan Province, P.R. China.
E-mail: liuzhangsuolzs@163.com

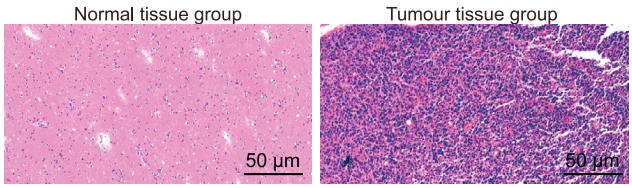

Figure 1. Histological Changes of Spinal Cord Glioma Tissues and Normal Tissues (200×)

Normal tissue group, normal spinal cord tissue; Tumor tissue group, spinal cord glioma tissue.

enables the release of Bak/Bax, which enables it to bind to anti-apoptotic Mcl-1 and A1, thus possessing a pro-apoptotic function.[12] Furthermore, an altered expression of PMAIP1 has been observed in numerous cancers, including colorectal cancer, breast cancer, and endometrial cancer.[13] LOC101928963, a novel lncRNA, was found to be differentially expressed in spinal cord glioma in its related chip data (GEO: GSE15824) downloaded from the GEO database. However, due to the limited literature that places a sufficient emphasis on the functional role of LOC101928963 in spinal cord glioma, this study is designed to investigate the potential of LOC101928963 in spinal cord glioma through the regulation of PMAIP1.

RESULTS

Spinal Cord Glioma Is Accompanied by Histological Changes

H&E staining was used to measure the histological deviations of the respective tissues. As the results indicated (Figure 1), cells in the spinal cord glioma tissue were observed to have exhibited disordered proliferation and abnormal changes in regard to cell morphology, while cells from the normal spinal cord tissue showed normal cell division, a uniform distribution, and no changes in cell morphology.

Loss of PMAIP1 Contributes to the Occurrence of Spinal Cord Glioma

To explore the role of PMAIP1 in spinal cord glioma, PMAIP1-positive expression was detected in spinal cord glioma tissue and normal spinal cord tissue by means of immunohistochemistry. PMAIP1 was mainly expressed in the cytoplasm and was represented by a yellowish-brown color after staining. The positive expression rate of PMAIP1 in the normal spinal cord tissue was confirmed to be 76.83%, while among the spinal cord glioma tissue, the associated figure was 52.05%. PMAIP1 exhibited decreased expression in the spinal cord glioma tissue, compared with the normal spinal cord tissue ($p < 0.05$) (Figure 2). These results suggested that the decrease in PMAIP1 played a crucial role in the occurrence of spinal cord glioma.

Spinal Cord Glioma Is Involved in Decrease of Cell Apoptosis

TUNEL assay was applied to detect the cell apoptosis of normal spinal cord tissue and spinal cord glioma tissue. As shown in Figure 3, the apoptotic-positive cells were brown in color; the AI of the normal spinal cord tissue was 45.15% ± 5.42%, while that of the spinal cord glioma tissue was 18.46% ± 2.10%. Thus, cell apoptosis was confirmed to be suppressed in cases of spinal cord glioma.

LOC101928963 Overexpression and PMAIP1 Downregulation Are Characterized in Spinal Cord Glioma

To explore the mechanism of LOC101928963 and PMAIP1 in spinal cord glioma, the expression of PMAIP1 was detected by qRT-PCR and western blot. In addition, the lncRNA LOC101928963 was verified using the GEO database (GEO: GSE15824). Compared to the normal spinal cord tissue, an elevation in the LOC101928963 expression was identified among the spinal cord glioma tissues (Figure 4A). The mRNA and protein expression of CyclinD2, CDK4, and Bcl-2 was increased, while the mRNA and protein expression of PMAIP1 and Bax was decreased in the spinal cord glioma tissue ($p < 0.05$) (Figures 4B–4D). These results suggested that LOC101928963 is overexpressed and that PMAIP1 is underexpressed in cases of spinal cord glioma.

PMAIP1 Is Negatively Regulated by LOC101928963

A dual-luciferase reporter assay was performed based on the correlation of LOC101928963 with PMAIP1. The results indicated that there were LOC101928963 binding sites in the PMAIP1 3′ UTR (Figure 5A). PMAIP1 is the target gene of LINC00936. The luciferase activity of the PMAIP1-Wt 3′ UTR was inhibited by the overexpression of LOC101928963, whereas it was increased after silencing LOC101928963 ($p < 0.05$), while the luciferase activity of the PMAIP1-Mut 3′ UTR was not affected by LOC101928963 ($p > 0.05$). These findings showed that LOC101928963 could specifically bind to PMAIP1 3′ UTR and downregulate the PMAIP1 gene expression at the post-transcriptional level (Figure 5B).

Silenced LOC101928963 Upregulates PMAIP1, Inhibits Cell Proliferation, and Promotes Cell Apoptosis in Spinal Cord Glioma

To explore the correlation shared between the relative mRNA and protein expression of LOC101928963, PMAIP1 and the proliferation- and apoptosis-related genes were all detected by means of qRT-PCR and western blot analysis. As depicted in Figure 6, no significant differences were identified in relation to the mRNA and protein expression between the blank and NC groups ($p > 0.05$). Compared with the blank and NC groups, LOC101928963 was overexpressed in the LOC101928963 vector and LOC101928963 vector + PMAIP1 vector groups; however, reductions were observed in the small interfering (si)-LOC101928963 and si-LOC101928963 + si-PMAIP1 groups ($p < 0.05$). The mRNA and protein expression of CyclinD2, CDK4, and Bcl-2 was elevated in the LOC101928963 vector and si-PMAIP1 groups, compared with the blank and NC groups; however, they were reduced in the si-LOC101928963 and PMAIP1 vector groups ($p < 0.05$). The mRNA and protein expression of PMAIP1 and Bax was downregulated in the LOC101928963 vector and si-PMAIP1 groups and increased in the si-LOC101928963 and PMAIP1 vector groups, compared with the blank and NC groups ($p < 0.05$). Compared with the si-LOC101928963 group, the mRNA and protein expression of CyclinD2, CDK4, and Bcl-2 was increased in the

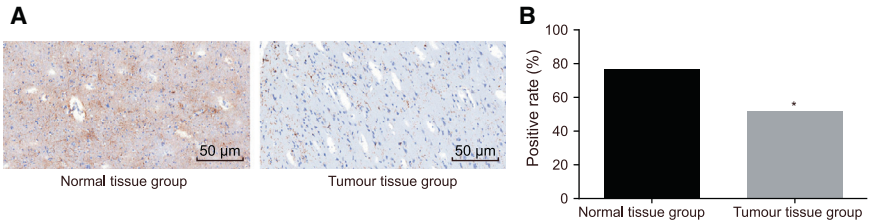

Figure 2. Spinal Cord Glioma Tissues Exhibits a Loss of PMAIP1

(A) PMAIP1-positive expression of normal spinal cord tissue and spinal cord glioma tissue, as detected by immunohistochemistry (200×). (B) Positive expression rate of PMAIP1 of normal spinal cord tissue and spinal cord glioma tissue. *p < 0.05, compared with the normal spinal cord tissue. Normal tissue group, normal spinal cord tissue; Tumor tissue group, spinal cord glioma tissue.

si-LOC101928963 + si-PMAIP1 group, with reduced mRNA and protein expression of PMAIP1 and Bax ($p < 0.05$). Compared with the LOC101928963 vector group, in the LOC101928963 vector + PMAIP1 vector group, the mRNA and protein expression of CyclinD2, CDK4, and Bcl-2 was downregulated, while the mRNA and protein expression of PMAIP1 and Bax was upregulated ($p < 0.05$). The results demonstrated that LOC101928963 inhibited the expression of PMAIP1, promoted the expression of cell-proliferation inducers, and inhibited the pro-apoptotic gene expression.

Silencing LOC101928963 or Overexpressing PMAIP1 Inhibits Cell Proliferation in Spinal Cord Glioma

To investigate the role of LOC101928963 and PMAIP1 in cell proliferation, an MTT assay was used to evaluate the cell proliferation among all groups. The results (Figure 7) indicated that the optical density (OD) values of the spinal cord and glioma cells among the 8 groups progressively increased over time. No significant differences were identified in relation to the OD values between the blank and NC groups at each time point ($p > 0.05$). Compared with the blank and NC groups, the rate of proliferation of glioma cells was increased in the LOC101928963 vector and si-PMAIP1 groups; however, decreases were identified in the si-LOC101928963 and PMAIP1 vector groups ($p < 0.05$). There were no significant differences detected in regard to the proliferation rate of glioma cells between the LOC101928963 vector + PMAIP1 vector and si-LOC101928963 + si-PMAIP1 groups ($p > 0.05$). Compared with that in the si-LOC101928963 group, the proliferation rate of glioma cells was elevated in the si-LOC101928963 vector + si-PMAIP1 group ($p < 0.05$). Comparisons made in regard to the LOC101928963 vector group suggested that the proliferation rate of glioma cells was decreased in the LOC101928963 vector + PMAIP1 vector group ($p < 0.05$). These results showed that LOC101928963 acted to promote cell proliferation in spinal cord glioma, while PMAIP1 exhibited an inhibitory effect on cell proliferation in spinal cord glioma.

Silencing LOC101928963 or Overexpressing PMAIP1 Induces Cell-Cycle Arrest and Apoptosis in Spinal Cord Glioma

The cell cycle and apoptosis among the groups were measured using propidium iodide (PI) staining and annexin V-FITC/PI staining to explore the effect of LOC101928963 on cell apoptosis. The results (Figure 8) indicated that there were no notable differences in relation to the cell-cycle distribution and apoptosis rate between the NC and blank groups ($p > 0.05$). Compared with the blank and NC groups, the number of cells at the G0/G1 phase was substantially decreased in the LOC101928963 vector and si-PMAIP1 groups with a significantly increased number at the S phase, which indicated that the apoptosis rate of glioma cells in the LOC101928963 vector and si-PMAIP1 groups had decreased, while the number of cells at the G0/G1 phase was substantially elevated in the si-LOC101928963 and PMAIP1 vector groups with a decreased number at the S phase; these findings suggested that the apoptosis rate of glioma cells was increased in the si-LOC101928963 and PMAIP1 vector groups ($p < 0.05$). There were no significant differences detected in the cell-cycle distribution and apoptosis rate between the LOC101928963 vector + PMAIP1 vector and si-LOC101928963 + si-PMAIP1 groups ($p > 0.05$). Compared with the si-LOC101928963 group, in the si-LOC101928963 + si-PMAIP1 group, the number of cells at the G0/G1 phase was significantly decreased with a significantly increased number at the S phase, which indicated that the apoptosis rate of glioma cells had decreased in the si-LOC101928963 + si-PMAIP1 group ($p < 0.05$). Compared with the LOC101928963 vector group, the number of cells at the G0/G1 phase was significantly elevated in the LOC101928963 vector + PMAIP1 vector group with

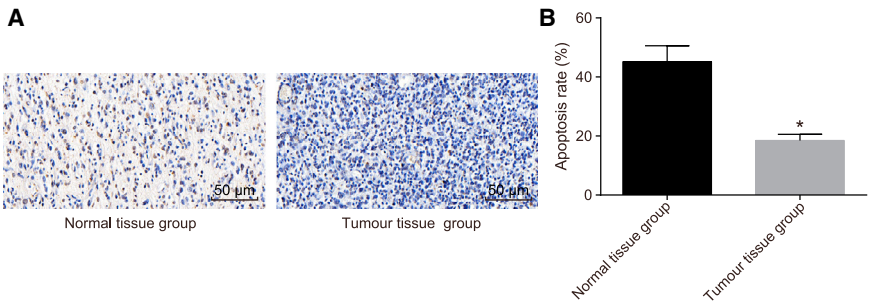

Figure 3. Decreased Cell Apoptosis Is Observed in Spinal Cord Glioma

(A) Cell apoptosis of normal spinal cord tissue and spinal cord glioma tissue (200×) detected by TUNEL assay. (B) AI of normal spinal cord tissue and spinal cord glioma tissue. *p < 0.05, compared with the normal spinal cord tissue. Normal tissue group, normal spinal cord tissue; Tumor tissue group, spinal cord glioma tissue.

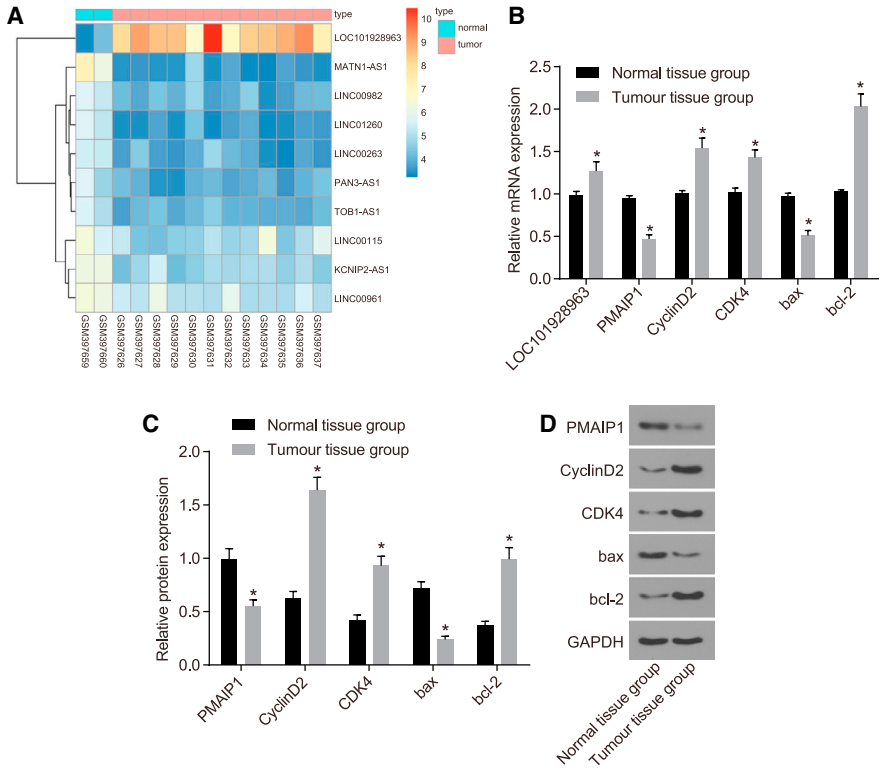

Figure 4. LOC101928963 Overexpression Is Detected in Spinal Cord Glioma

(A) LOC101928963 overexpression in spinal cord glioma in chip data (GEO: GSE15824). (B) Relative mRNA expression of PMAIP1, CyclinD2, CDK4, Bax, and Bcl-2 in spinal cord glioma tissue, as determined by qRT-PCR. (C) Relative protein expression of PMAIP1, CyclinD2, CDK4, Bax, and Bcl-2 spinal cord glioma tissue, as detected by western blot analysis. (D) Gray values of PMAIP1, CyclinD2, CDK4, Bax, and Bcl-2 protein bands. *$p < 0.05$, compared with the normal spinal cord tissue. Normal tissue group, normal spinal cord tissue; Tumor tissue group, spinal cord glioma tissue.

a decreased number at the S phase, which indicated that the apoptosis rate was increased in the LOC101928963 vector + PMAIP1 vector group ($p < 0.05$). These results showed that LOC101928963 could inhibit the apoptosis of glioma cells, while PMAIP1 could promote the apoptosis of glioma cells.

DISCUSSION

Spinal cord glioma is an infrequently occurring tumor observed particularly among children and accounts for less than 10% of all CNS tumors.[5] However, due to the scarcity of data and the devastating consequences, spinal cord glioma is difficult to manage.[2] Therefore, urgent elucidation is required in regard to the finer molecular mechanisms of the disease. lncRNAs have been reported to share a close correlation with various cancers, in addition to acting as cancer suppressors and oncogenes in different cancers.[9] A previous study highlighted that lncRNAs are unexploited resources for the development of cancer diagnosis and treatment.[14] Thus, a key objective of this study was to investigate the role of the lncRNA LOC101928963 in spinal cord glioma and the correlation between LOC101928963 and PMAIP1. Furthermore, our findings indicated that a low expression of LOC101928963 inhibits cell proliferation and promotes cell apoptosis by upregulating PMAIP1 in spinal cord glioma.

Various lncRNAs, such as MEG3 and CRNDE, have been observed to be correlated with glioma and played a key role in carcinogenesis, differentiation, and the development of glioma.[15–17] Another lncRNA, H19, was also found to be upregulated in glioma, which could promote cell invasion in glioma.[18] In this study, LOC101928963 was shown to be overexpressed, while PMAIP1 was underexpressed in spinal cord glioma. Through target prediction, PMAIP1 was shown to be a target of LOC101928963. PMAIP1, also referred to as NOXA, was extremely discrepant in mantle cell lymphoma cells.[19] PMAIP1 has been specified to be poorly expressed in various cancers, such as breast cancer, lung cancer, and castration-resistant prostate cancer.[20–22] It has been previously explained that the upregulation of PMAIP1 could antagonize tumorigenesis by inducing cell death in glioma.[23,24] Moreover, the luciferase activity detection in response to the overexpression or silencing of LOC101928963 further verified that PMAIP1 could be negatively regulated by LOC101928963. In this regard, we speculate that LOC101928963 may function in the development of spinal cord glioma through the regulation of PMAIP1.

The obtained results of the present functional experiments highlighted that cell proliferation was promoted, while cell apoptosis was inhibited after cells were transfected with overexpressed

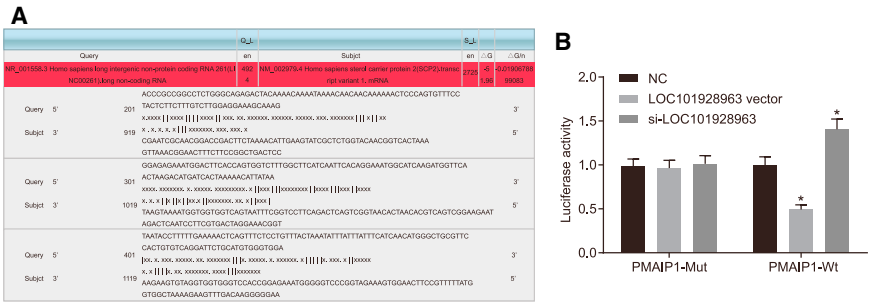

Figure 5. PMAIP1 Is a Target Gene of LOC101928963

(A) The predicted consequential pairing of LOC101928963 and PMAIP1. (B) Relative luciferase activity determined by dual-luciferase reporter gene assay in the NC, LOC101928963 vector, and si-LOC101928963 groups. *p < 0.05, compared with the NC group; NC, negative control; Subjct, subject.

LOC101928963 or small interfering RNA (siRNA) targeting PMAIP1, corresponding to increased CyclinD2, CDK4, and bcl-2 expression and decreased PMAIP1 and Bax expression. It has been reported that the loss of PMAIP1 plays a role in tumorigenesis and development.[25] As a member of the D-type cyclins, CyclinD2 plays a pivotal role in the progression of the cell cycle.[26] Moreover, CDK4 has been reported to be activated by D-type cyclins.[27] Importantly, CDKs promote cell-cycle progression to the S phase through its binding action on cyclins.[28] It is reported that PMAIP1 is a pro-apoptotic factor whose activation contributes to the accumulation of anti-apoptotic MCL1 and neutralizes the effect of the anti-apoptotic protein Bcl-2l1/Bcl-xl.[29] A former study that focused on acute myelogenous leukemia provided evidence verifying that the up-regulation of the PMAIP1 gene triggers cell apoptosis,[30] which was largely consistent with the results of our study. Furthermore, PMAIP1 overexpression was demonstrated to inhibit cell proliferation, while PMAIP1 silencing promotes cell-growth recovery.[31] Based on the results of our cellular experiments, we conclude that LOC101928963 enhances spinal cord glioma cell proliferation and inhibits cell apoptosis via downregulating PMAIP1.

Collectively, the results of the present study indicate that the silencing of LOC101928963 can result in the upregulation of PMAIP1, which induced the inhibition of cell proliferation and promotion of cell apoptosis in spinal cord glioma. The present study and its results provide innovative insights into a potentially promising clinical treatment approach, providing a fresh perspective for targeted therapy and the development of targeted drugs for spinal cord glioma. P53, widely known as a tumor suppressor involved in cell-cycle arrest and the transcriptional activation of p21, has been reported to increase PMAIP1 in response to DNA damage.[32,33] A study also indicated the function of PMAIP1 in the regulation of a p53-mediated apoptotic pathway.[34] To fully validate the results of the present study and contribute to the development and management of spinal cord glioma treatment, further studies and clinical validation for a potential regulatory network of PMAIP1, LOC101928963, and the p53 signaling pathway are required in the future.

MATERIALS AND METHODS

Ethical Statement

All tissue sample collection was performed after written informed consent was obtained from the patients and their respective families. In addition, the study was conducted with the approval of the Ethics Committee of The Tumor Hospital of the First Affiliated Hospital of Zhengzhou University.

lncRNA Screening

The spinal-glioma-related chip data (GEO: GSE15824) and annotated probe files were downloaded from the GEO database (https://www.ncbi.nlm.nih.gov/geo) and were detected using the Affymetrix Human Genome U133 Plus 2.0 Array. The Affy installation package of R software was used for background correction and normalization of the chip data.[35] This study used a nonspecific filtering method on the expression profile data, while screening out the differential expression of lncRNAs was performed using the linear model and empirical Bayes statistics method in the limma installation package combined with traditional t tests.

Study Subjects

Eighty-two spinal cord glioma patients who were previously diagnosed at the Department of Neurosurgery of The Tumor Hospital of the First Affiliated Hospital of Zhengzhou University between January 2014 and January 2017 were selected for the purposes of this study. The patient pool consisted of 47 males and 35 females. All diagnoses were confirmed by operative and pathology means. The patients' ages ranged from 6 to 72 years, with a mean age of 39 years. All patients showed varying degrees of sensory disturbance, 11 cases underwent monoplegia, 21 cases exhibited paralysis of their lower extremities, 15 cases displayed incomplete paralysis of their limbs, 9 cases suffered from dyspnea, and 26 cases had difficulty with urination and defecation. Tumors were located in the cervical region in 20 cases, the thoracic region in 23 cases, and the lumbar region in 39 cases. According to the World Health Organization (WHO) classification of tumors, the tumor types include 36 cases of ependymomas, 7 cases of anaplastic ependymoma, 19 cases of WHO grade II astrocytomas (AII), 11 cases of WHO grade III anaplastic astrocytomas (AAIII), and 9 cases of WHO grade III oligoastrocytomas (OAIII).[1] The inclusion criteria were as follows: (1) patients had been diagnosed with spinal cord glioma by means of histopathology or cytology; (2) all patients underwent enhanced MRI scans prior to operation; (3) patients underwent initial treatment procedures that did not include chemotherapy (CT) and/or radiotherapy (RT); (4) patients had measurable or assessable lesions; (5) patients had normal routine blood tests and functioning vital organs, including the heart, liver, and kidney; and (6) the estimated life expectancy of the

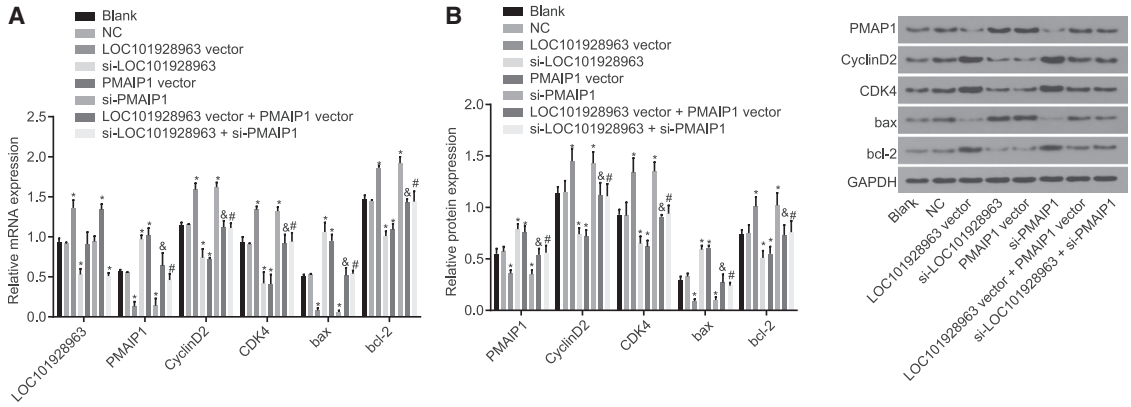

Figure 6. LOC101928963 Downregulates PMAIP1 to Promote Cell Proliferation and Inhibit Cell Apoptosis

(A) Relative mRNA expression of LOC101928963, PMAIP1, CyclinD2, CDK4, Bax, and Bcl-2 of spinal cord glioma cells, as determined by qRT-PCR. (B) Relative protein expression of PMAIP1, CyclinD2, CDK4, Bax, and Bcl-2 of spinal cord glioma cells, as measured by western blot analysis. (C) Gray values of PMAIP1, CyclinD2, CDK4, Bax, and Bcl-2 protein bands of spinal cord glioma cells. *$p < 0.05$, compared with the blank and NC groups; &$p < 0.05$, compared with the LOC101928963 vector group; #$p < 0.05$, compared with the si-LOC101928963 group. NC, negative control.

patients exceeded 3 months. The exclusion criteria used were as follows: (1) patients suffered from other neurological disorders or severe systemic diseases at the same time; (2) female patients were currently pregnant or lactating; (3) patients were undergoing treatment for other malignancies; (4) patients had severely damaged functions of their vital organs; (5) patients had a history of autoimmune disease; (6) patients were in the active phase of a chronic infection or suffering from an acute infectious disease; (7) patients had an allergic constitution or a clear history of drug allergy; or (8) patients were currently undergoing other clinical trials at the same time. An additional 73 cases of normal spinal cord tissue were obtained from patients who accepted surgical decompression for acute spinal cord injuries at The Tumor Hospital of the First Affiliated Hospital of Zhengzhou University. These patients were included in the normal group. Each tissue sample was conserved in a refrigerator at −80°C.

H&E Staining

The frozen spinal cord glioma tissues and normal spinal cord tissues were fixed in 4% paraformaldehyde for 24 h. The tissues were then dehydrated by 80%, 90%, and 100% ethanol and butanol, respectively, followed by a waxing process in a wax box at 60°C. Tissues were embedded and sliced into 5-μm serial sections, followed by extension at 45°C and drying at 60°C for 1 h. After being dewaxed in xylene and hydrated, the sections were stained with H&E (Beijing Solarbio Science & Technology, Beijing, China), dehydrated by graded ethanol, cleared in xylene, and mounted with neutral balsam. The histopathological changes of the spinal cord glioma tissues and normal spinal cord tissues were analyzed using an optical microscope (XP-330, Shanghai Bingyu Optical Instrument, Shanghai, China).

Immunohistochemistry

Spinal cord glioma tissue and normal spinal cord tissue were fixed in 10% formalin, embedded in paraffin, and then sliced into 3- to 4-μm sections. The sections were immersed in 3% H_2O_2; dewaxed in xylene I and xylene II (each for 10 min); dehydrated with graded ethanol of 100%, 95%, 80% and 70% (2 min each time); and then washed twice with distilled water (5 min each time) in a shaker. The sections were subsequently soaked in 3% H_2O_2 for 10 min and washed with distilled water, followed by antigen repair at high pressure for 90 s. After being cooled at room temperature, the sections were washed using PBS, blocked with 5% BSA at 37°C for 30 min, and then incubated with mouse anti-human PMAIP1 monoclonal antibody (1:300; ab36833, Abcam, Cambridge, MA, USA) overnight at 4°C. The sections were incubated with biotinylated goat anti-mouse immunoglobulin G-horseradish peroxidase (IgG-HRP) secondary antibody (SE134, Beijing Solarbio Science & Technology, Beijing, China) at 37°C for 30 min. The sections were subsequently counterstained by hematoxylin (C0105, Beyotime Biotechnology, Shanghai, China) for 30 s and developed using 3,3-diaminobenzidine (DAB; chromogenic agent, P0202; Beyotime Biotechnology, Shanghai, China). The samples were then dehydrated in hydrochloric acid-ethanol, cleared, and mounted by neutral balsam. The sections were observed and photographed under a microscope. Cells with brownish-yellow cytoplasm were determined to be PMAIP1-positive cells.[36] The proportion of positive cells was regarded as the positive expression rate of the total amount of cells. Five fields of vision under a high power lens of each section were randomly selected to observe the positive expression rate and the localization of positive expression in tissues. The experiment was conducted three times.

TUNEL Assay

Paraffin sections of spinal cord glioma tissues and normal spinal cord tissues were dewaxed in xylene I and xylene II (each for 10 min) and dehydrated in graded ethanol of 100%, 95%, 80%, and 70%, respectively (2 min each time). The sections were then washed 3 times with PBS (each time for 5 min), cultured with proteinase K solution at 37°C for 30 min, and again washed 3 times with PBS (each time for 5 min), followed by fixation with 4% paraformaldehyde for 2 h. After 3 subsequent PBS washes (each time for 5 min), the sections

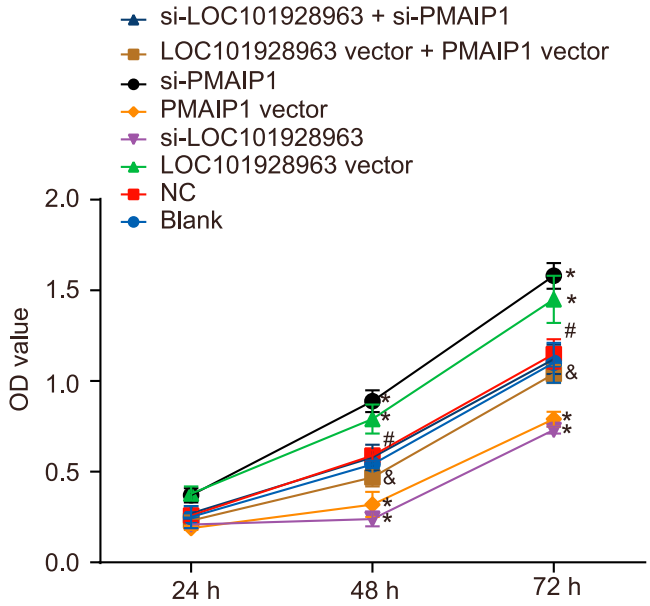

Figure 7. Cell Proliferation Is Enhanced by LOC101928963 Overexpression or PMAIP1 Downregulation

*p < 0.05, compared with the blank and NC groups; &p < 0.05, compared with the LOC101928963 vector group; #p < 0.05, compared with the si-LOC101928963 group. NC, negative control.

were blocked in methanol that contained 3% H_2O_2 for 10 min. The sections were then washed 3 times with PBS (5 min each time) and cultured in 20% sucrose phosphate buffer overnight at 4°C. The next day, the samples were sliced into 20-μm serial sections at −22°C using a slice machine. Ten sections were obtained from each tissue sample for terminal deoxynucleotidyl transferase (TDT)-mediated dUTP-biotin nick end-labeling (TUNEL) staining using a TUNEL kit (Boehringer Mannheim, Mannheim, Germany), according to the manufacturer's protocol. The stained samples were observed under an optical microscope (Leica DM4 P, Shanghai Meijing Electronics, Shanghai, China), with the cells that exhibited dark particles considered to be apoptotic cells. Ten fields of vision under a high-power lens (200×) were randomly selected from each sample to count the number of apoptotic cells and the number of total cells. The proportion of apoptotic cells among the total number of cells was regarded as the AI. The experiment was conducted three times to obtain the mean value.

qRT-PCR

TRIzol reagent (1 mL; Invitrogen Life Technologies, Carlsbad, CA, USA) was added to the spinal cord glioma, as well as the normal spinal cord tissue, respectively, after which they were crushed in an ice bath. Total RNA was extracted based on the method provided by the manufacturer's protocol for TRIzol reagent. The purity and concentration of RNA were measured by UV spectrophotometry (UV1901, Shanghai AuCy Technology Instrument, Shanghai, China). Samples with an A260/A280 that ranged from 1.8 to 2.0 were adjusted to a concentration of 50 ng/μL, and total RNA was reversely transcribed into cDNA using a PrimeScript RT Reagent Kit (Takara, RR047A, BeiJing Think-Far Technology, Beijing, China). Next, cDNA was conserved at −80°C. The primers (shown in Table 1) were designed by GeneTools software and synthesized by Beijing Tsingke Biological Technology (Beijing, China). qRT-PCR was subsequently performed using an ABI PRISM 7900HT apparatus based on a two-step method. U6 was used as the internal reference of LOC101928963, while glyceraldehyde-3-phosphate dehydrogenase (GAPDH) was referred to as the internal reference of the other genes in the experiment. The reaction conditions were as follows: predenaturation at 95°C for 30 s, followed by 40 cycles of denaturation at 95°C for 5 s, annealling at 58°C for 30 s, and extension at 72°C for 15 s. The relative mRNA expression of LOC101928963, PMAIP1, CyclinD2, CDK4, Bax, and Bcl-2 were calculated using the $2^{-\Delta\Delta Ct}$ method. Each gene from each sample was set up with 3 duplicated wells. This method was also applied for the subsequent cell experiments. The experiment was conducted in triplicate.

Western Blot

Tissue samples were ground to a uniform powder at a low temperature, washed 3 times with PBS, lysed with protein lysate, and centrifuged for 20 min at 12,000 rpm, followed by the collection of the supernatant. The protein concentration was determined using a bicinchoninic acid (BCA) protein assay kit (P0012-1, Beyotime Institute of Biotechnology, Shanghai, China). Cells in the logarithmic growth phase were centrifuged at 3,000 rpm at 4°C for 20 min. After removal of the supernatant, the packed cell volume (PCV) was estimated accordingly. The cells were treated with 100 μL lysis buffer and 1 μL enzyme inhibitor (1111111, Roche, Beijing Jiamay Biotechnology Co., Ltd., Beijing, China) per 20 μL PCV for 30 min on ice and centrifuged at 12,000 rpm for 10 min at low temperature. The supernatant protein was then obtained for western blot purposes. Protein samples (50 μg) were dissolved in 2× SDS loading buffer, boiled at 100°C for 5 min, separated on 10% SDS-PAGE, and transferred onto a polyvinylidene fluoride (PVDF) membrane. The membranes were then blocked using 5% skim milk at room temperature for 1 h, followed by PBS washing for 2 min. The membranes were subsequently incubated with diluted mouse anti-human primary antibodies of PMAIP1 (1:1,000, ab140129), CyclinD2 (1:1,000, ab207604), CDK4 (1:1,000, ab108357), Bax (1:1,000, ab32503), Bcl-2 (1:1,000, ab119506), and GAPDH (1:500, ab8245). These antibodies were purchased from Abcam (Cambridge, MA, USA). The membrane was washed using TBST 3 times, incubated with the second antibody of HRP-labeled goat anti-mouse IgG (1:5,000) for 1 h, and rinsed 3 times using TBST (5 min each time). An enhanced chemiluminescence (ECL) kit was used for development. The liquid was subsequently removed, with the samples exposed to X-rays and photographed accordingly. The gray value of the bands was analyzed using a gel imaging analysis system. GAPDH was used as the internal reference. The average absorbance ratio of the target protein band to the internal reference band was considered to be the relative protein expression. A statistical analysis chart was designed according to the

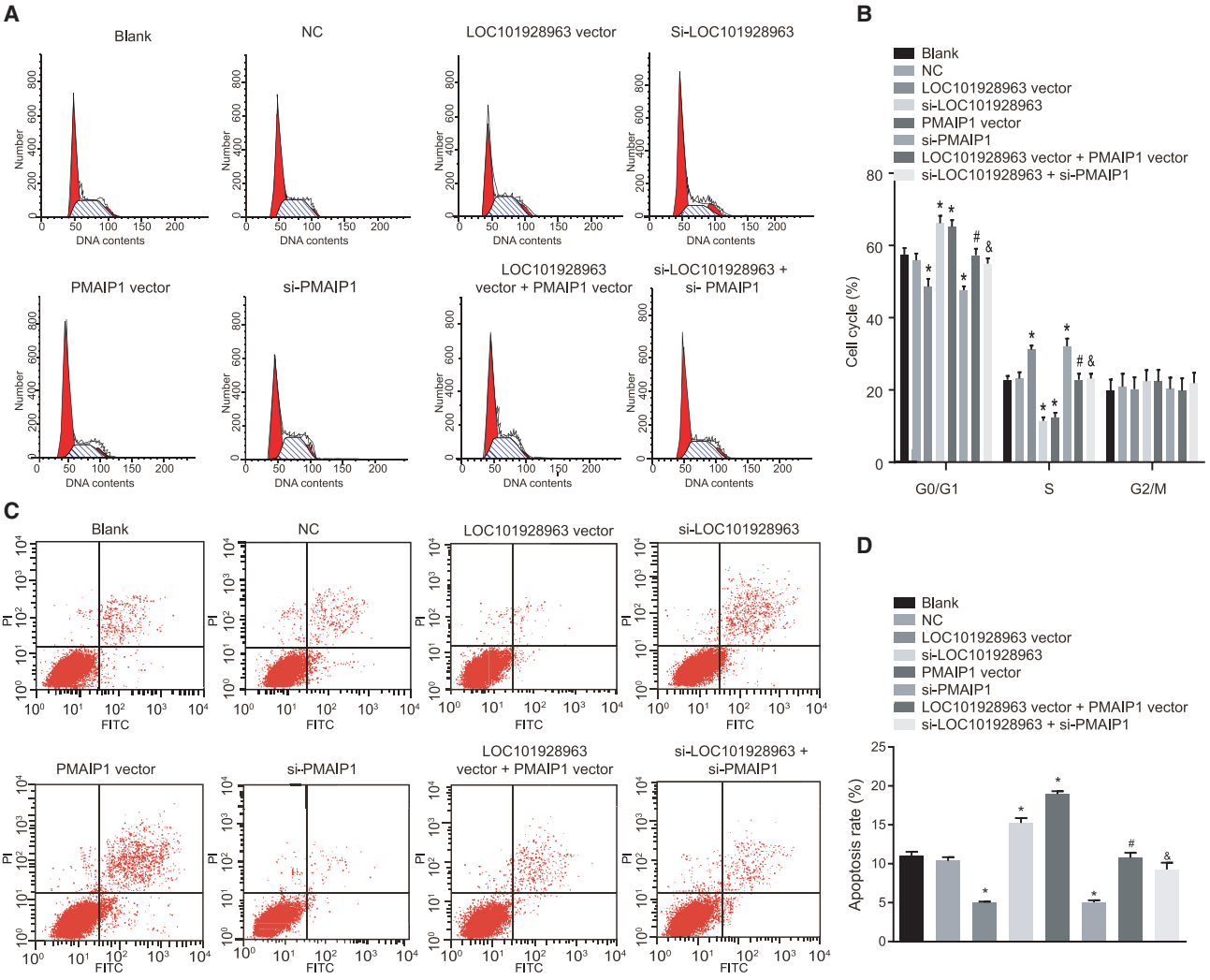

Figure 8. LOC101928963 Overexpression Arrests Cells in S Phase and Represses Cell Apoptosis

(A) Cell-cycle distribution after transfection, as assessed by PI staining. (B) Histogram comparing the cell-cycle distribution after transfection. (C) Cell apoptosis mapping after transfection, as assessed by annexin V-FITC/PI staining. (D) Cell apoptosis rate after transfection. *$p < 0.05$, compared with the blank and NC groups; $^{\&}p < 0.05$, compared with the LOC101928963 vector group; $^{\#}p < 0.05$, compared with the si-LOC101928963 group. NC, negative control.

relative protein expression of the protein samples. The experiment was conducted three times.

Dual Luciferase Reporter Gene Assay

A biology prediction website[37] was used to analyze the target gene of lncRNA LOC101928963. A dual luciferase reporter gene assay was used to verify whether the PMAIP1 was the target gene of LOC101928963. HEK293T cells (AT-1592, American Type Culture Collection, Manassas, VA, USA) were inoculated in a 24-well plate and cultured for 24 h. The complementary mutation sites of the PMAIP1 wild-type (WT) target sequence were designed, and the target fragment was inserted into the pMIR-reporter plasmid by restriction endonuclease digestion using SpeI and Hind III and ligated using T4 DNA ligase. The luciferase reporter gene vector of PMAIP1 (pmiRRB-PMAIP1-3′ UTR) was constructed. The sequenced dual luciferase reporter gene vectors that carried WT and mutant-type (Mut) sequences were separately cotransfected with LOC101928963 vector, siRNA-LOC101928963, and negative control (NC) into the HEK293T cells. At 48 h after transfection, the culture medium was removed. The cells were washed twice with PBS, collected, and lysed. The luciferase reporter activity was measured by the Dual-Luciferase Reporter Assay System (E1910, Promega Biotech, Madison, WI, USA). Then, 10 μL cells were combined with 50 μL firefly luciferase to determine the firefly luciferase activity, and 50 μL Renilla luciferase was added to determine the Renilla luciferase activity. The relative luciferase reporter activity was considered to be the ratio of the firefly luciferase activity to the Renilla luciferase activity. The experiment was conducted three times.

Table 1. The Primer Sequences for qRT-PCR

Gene	Sequence
LOC101928963	F: 5′-AAGGAACCGGAAGTGTCGTG-3′ R: 5′-ATTCCCTCCTCCAGTCGTA-3′
PMAIP1	F: 5′-CATGAGGGGACTCCTTCAAA-3′ R: 5′-TTCCATCTTCCGTTTCCAAG-3′
CyclinD2	F: 5′-TCATGACTTCATTGGAGCA-3′ R: 5′-CACTTCCTCATCCTGCTG-3′
CDK4	F: 5′-CATGTAGACCAGGACCTAAGC-3′ R: 5′-AACTGGCGCATCAGATCCTAG-3′
Bax	F: 5′-TTTGCTTCAGGGTTTCATCC-3′ R: 5′-CAGTTGAAGTTGCCGTCAGA-3′
Bcl-2	F: 5′-GCATGCCTTTGTGGAACTGT-3′ R: 5′-AGCCTGCAGCTTTGTTTCAT-3′
GAPDH	F: 5′-CGACCACTTTGTCAAGCTCA-3′ R: 5′-AGGGGTCTACATGGCAACTG-3′
U6	F: 5′-CTCGCTTCGGCAGCACA-3′ R: 5′-AACGCTTCACGAATTTGCGT-3′

F, forward; R, reverse.

Cell Transfection and Grouping

Human astrocytoma cells (U87R-DOX; FS-001-0642, Shanghai Fusheng Industrial, Shanghai, China) were cultured with RPMI 1640 culture medium that contained 15% fetal bovine serum (FBS) at 37°C in a 5% CO_2 incubator with saturation humidity. The culture medium was replaced at 2- to 3-day intervals according to the growth of the cells. Single-layer cells were incubated to approximately 80%–90% confluence and then passaged.

Cells at the logarithmic growth phase were divided into blank (without treatment), NC (transfected with unrelated sequence), LCO101928963 vector (transfected with overexpressed LOC101928963 sequence), si-LOC101928963 (transfected with siRNA targeting LOC101928963), PMAIP1 vector (transfected with overexpressed PMAIP1 sequence), si-PMAIP1 (transfected with siRNA targeting PMAIP1), LOC101928963 vector + PMAIP1 vector (cotransfected with overexpressed LOC101928963 and overexpressed PMAIP1), and si-LOC101928963 + si-PMAIP1 groups (cotransfected with si-LOC101928963 and si-PMAIP1). Prior to transfection, cells at the logarithmic growth phase were inoculated into a 6-well plate. When the density had reached approximately 80%–90% confluence, the cells were transferred to serum-free Opti-MEM (GIBCO-BRL, Grand Island, NY, USA). Transfection was conducted according to the instructions of the Lipofectamine 2000 (lipo) kit (Invitrogen Life Technology, Carlsbad, CA, USA). The lipo solution (11668-027, Shanghai Kanwin Biotechnology, Shanghai, China) contained 240 μL serum-free medium and 10 μL lipo with a total volume of 250 μL and was incubated for a period of 5 min. The plasmid solution contained 200 μL serum-free medium and 50 μg plasmid, with a total volume of 250 μL. The two solutions were mixed, allowed to rest at room temperature for 20 min, and then transferred to the wells by dropwise means, followed by gentle shaking of the plate. Cells were cultured at 37°C in a 5% CO_2 incubator for 5–6 h. The medium was subsequently replaced with a complete medium, and the cells were incubated for 24–48 h, in preparation for the following experiment.

MTT Assay

After a 24-h period of transfection, cells in the logarithmic growth phase were cultured in DMEM that contained 10% FBS to prepare a cell suspension of 1×10^4 cells/mL. The cell suspension was inoculated in a 96-well plate with 8 wells (each, 100 μL) for each group and placed in a 5% CO_2 incubator at 37°C. The cells were added with 5 mg/mL MTT solution (Sigma-Aldrich, St. Louis, MO, USA) at 24, 48, and 72 h, following a 4-h period of culturing, and the supernatant was then discarded. Next, 150 μL DMSO was added to each well and shaken for 10 min. The OD values of each well were measured at the wavelength of 490 nm by an automatic enzyme reader (Bio-Rad Laboratories, Hercules, CA, USA). The experiment was conducted three times.

Flow Cytometry

The culture medium was discarded 48 h after transfection. The cells were washed once with PBS, treated with 0.25% trypsin, collected, and centrifuged at 1,000 rpm for 5 min at 4°C with the supernatant discarded. The cells were then washed twice using precooled balanced PBS and centrifuged at 1,000 rpm for 5 min with the supernatant discarded. The cells were then fixed in precooled 70% ethanol at 4°C overnight. After being rinsed twice with PBS, the cells were centrifuged at 1,000 rpm for 5 min and added with 10 μL RNase for incubation at 37°C for 5 min. The cells were stained using 1% PI (40710ES03, Shanghai Qcbio Science & Technologies, Shanghai, China) under dark conditions for 30 min. The red fluorescence at the 488-nm excitation wavelength was recorded using a BD FACSCalibur flow cytometer (BD Biosciences, Franklin Lakes, NJ, USA) for cell-cycle detection. The experiment was conducted three times.

At 48 h after transfection, the cells were digested by trypsin without EDTA, collected, and centrifuged at 1,000 rpm for 5 min at 4°C with the supernatant discarded. The cells were washed using precooled PBS and centrifuged at 1,000 rpm for 5 min, followed by the discarding of the supernatant. An annexin-V-FITC/PI kit (CA1020, Beijing Solarbio Science & Technology, Beijing, China) was used to detect cell apoptosis. Cells were washed with binding buffer, resuspended in annexin-V-FITC/binding buffer (1:40), mixed, and incubated at room temperature for 30 min. The cells were then resuspended in annexin-V-FITC/binding buffer (1:40), mixed, and cultured at room temperature for 15 min. A flow cytometer was used to detect the cell apoptosis. In the fluorescence dot plot histogram of annexin-V/PI-stained cells (Figure 8C), the left lower quadrant shows normal viable cells, which are annexin V−/PI−, and the right lower quadrant displays early-apoptotic cells, which are annexin V+/PI−. The left upper quadrant exhibits necrotic cells, which are positive for annexin V−/PI+, while the right upper quadrant displays late-apoptotic cells and secondary necrosis cells, which are annexin V+/PI+. The experiment was conducted three times.

Statistical Analysis

All data were analyzed using SPSS v.21.0 statistical software (IBM, Armonk, NY, USA). Measurement data were expressed as the mean ± SD. Comparisons between two groups were conducted by t tests. Comparisons among multiple groups were assessed by one-way ANOVA. $p < 0.05$ was considered to be statistically significant.

AUTHOR CONTRIBUTIONS

Conception and design: D.-K.Y., J.W., and J.-Y.Z.; analysis and interpretation: Z.-S.L., Y.-J.Z., and T.-S.L.; data collection: D.-K.Y., J.W., and J.-Y.Z.; writing the article: Z.-S.L., Y.-J.Z., and T.-S.L.; critical revision of the article: D.-K.Y., J.W., and J.-Y.Z.; final approval of the article: Z.-S.L., Y.-J.Z., and T.-S.L.; statistical analysis: D.-K.Y., J.W., and J.-Y.Z.; obtained funding: Z.-S.L., Y.-J.Z., and T.-S.L.

CONFLICTS OF INTEREST

The authors declare no competing interests.

ACKNOWLEDGMENTS

We extend our sincere appreciation to the reviewers for their helpful comments on this article. The datasets generated/analyzed during the present study are available.

REFERENCES

1. Crowley, R.W., Burke, R.M., Lopes, M.B.S., Hamilton, D.K., and Jane, J.A., Sr. (2015). Long-term cure of high-grade spinal cord glioma in a pediatric patient who underwent cordectomy. J. Neurosurg. Spine *23*, 635–641.

2. Milano, M.T., Johnson, M.D., Sul, J., Mohile, N.A., Korones, D.N., Okunieff, P., and Walter, K.A. (2010). Primary spinal cord glioma: a Surveillance, Epidemiology, and End Results database study. J. Neurooncol. *98*, 83–92.

3. Haresh, K.P., Chinikkatti, S.K., Prabhakar, R., Rishi, A., Rath, G.K., Sharma, D.N., and Julka, P.K. (2008). A rare case of intradural extramedullary Ewing's sarcoma with skip metastasis in the spine. Spinal Cord *46*, 582–584.

4. Rissi, D.R., Barber, R., Burnum, A., and Miller, A.D. (2017). Canine spinal cord glioma. J. Vet. Diagn. Invest. *29*, 126–132.

5. Khalil, J., Chuanying, Z., Qing, Z., Belkacémi, Y., and Mawei, J. (2017). Primary spinal glioma in children: Results from a referral pediatric institution in Shanghai. Cancer Radiother. *21*, 261–266.

6. Seki, T., Hida, K., Yano, S., Aoyama, T., Koyanagi, I., and Houkin, K. (2015). Surgical outcomes of high-grade spinal cord gliomas. Asian Spine J. *9*, 935–941.

7. Chen, Y., Wu, J.J., Lin, X.B., Bao, Y., Chen, Z.H., Zhang, C.R., Cai, Z., Zhou, J.Y., Ding, M.H., Wu, X.J., et al. (2015). Differential lncRNA expression profiles in recurrent gliomas compared with primary gliomas identified by microarray analysis. Int. J. Clin. Exp. Med. *8*, 5033–5043.

8. Zhang, T., Wang, Y.R., Zeng, F., Cao, H.Y., Zhou, H.D., and Wang, Y.J. (2016). LncRNA H19 is overexpressed in glioma tissue, is negatively associated with patient survival, and promotes tumor growth through its derivative miR-675. Eur. Rev. Med. Pharmacol. Sci. *20*, 4891–4897.

9. Li, J., Zhang, M., An, G., and Ma, Q. (2016). LncRNA TUG1 acts as a tumor suppressor in human glioma by promoting cell apoptosis. Exp. Biol. Med. (Maywood) *241*, 644–649.

10. Huang, K., Sun, J., Yang, C., Wang, Y., Zhou, B., Kang, C., Han, L., and Wang, Q. (2017). HOTAIR upregulates an 18-gene cell cycle-related mRNA network in glioma. Int. J. Oncol. Published online March 17, 2017. https://doi.org/10.3892/ijo.2017.3901.

11. Zhao, X., Liu, X., and Su, L. (2014). Parthenolide induces apoptosis via TNFRSF10B and PMAIP1 pathways in human lung cancer cells. J. Exp. Clin. Cancer Res. *33*, 3.

12. Idrus, E., Nakashima, T., Wang, L., Hayashi, M., Okamoto, K., Kodama, T., Tanaka, N., Taniguchi, T., and Takayanagi, H. (2011). The role of the BH3-only protein Noxa in bone homeostasis. Biochem. Biophys. Res. Commun. *410*, 620–625.

13. Kapoor, S. (2008). Altered expression of the PMAIP1 gene: A major player in the evolution of gastrointestinal and systemic malignancies. Dig. Dis. Sci. *53*, 2834–2835.

14. Gibb, E.A., Brown, C.J., and Lam, W.L. (2011). The functional role of long non-coding RNA in human carcinomas. Mol. Cancer *10*, 38.

15. Wang, P., Ren, Z., and Sun, P. (2012). Overexpression of the long non-coding RNA MEG3 impairs in vitro glioma cell proliferation. J. Cell. Biochem. *113*, 1868–1874.

16. Wang, Y., Wang, Y., Li, J., Zhang, Y., Yin, H., and Han, B. (2015). CRNDE, a long-noncoding RNA, promotes glioma cell growth and invasion through mTOR signaling. Cancer Lett. *367*, 122–128.

17. Zhang, X., Sun, S., Pu, J.K., Tsang, A.C., Lee, D., Man, V.O., Lui, W.M., Wong, S.T., and Leung, G.K. (2012). Long non-coding RNA expression profiles predict clinical phenotypes in glioma. Neurobiol. Dis. *48*, 1–8.

18. Shi, Y., Wang, Y., Luan, W., Wang, P., Tao, T., Zhang, J., Qian, J., Liu, N., and You, Y. (2014). Long non-coding RNA H19 promotes glioma cell invasion by deriving miR-675. PLoS ONE *9*, e86295.

19. Dengler, M.A., Weilbacher, A., Gutekunst, M., Staiger, A.M., Vöhringer, M.C., Horn, H., Ott, G., Aulitzky, W.E., and van der Kuip, H. (2014). Discrepant NOXA (PMAIP1) transcript and NOXA protein levels: a potential Achilles' heel in mantle cell lymphoma. Cell Death Dis. *5*, e1013.

20. Wang, P., Yu, W., Hu, Z., Jia, L., Iyer, V.R., Sanders, B.G., and Kline, K. (2008). Involvement of JNK/p73/NOXA in vitamin E analog-induced apoptosis of human breast cancer cells. Mol. Carcinog. *47*, 436–445.

21. Zhou, W., Xu, J., Li, H., Xu, M., Chen, Z.J., Wei, W., Pan, Z., and Sun, Y. (2017). Neddylation e2 ube2f promotes the survival of lung cancer cells by activating crl5 to degrade noxa via the k11 linkage. Clin. Cancer Res. *23*, 1104–1116.

22. Wei, X., Zhou, P., Lin, X., Lin, Y., Wu, S., Diao, P., Xie, H., Xie, K., and Tang, P. (2014). MLN2238 synergizes BH3 mimetic ABT-263 in castration-resistant prostate cancer cells by induction of NOXA. Tumour Biol. *35*, 10213–10221.

23. Foster, K.A., Jane, E.P., Premkumar, D.R., Morales, A., and Pollack, I.F. (2015). NVP-BKM120 potentiates apoptosis in tumor necrosis factor-related apoptosis-inducing ligand-resistant glioma cell lines via upregulation of Noxa and death receptor 5. Int. J. Oncol. *47*, 506–516.

24. Premkumar, D.R., Jane, E.P., Agostino, N.R., DiDomenico, J.D., and Pollack, I.F. (2013). Bortezomib-induced sensitization of malignant human glioma cells to vorinostat-induced apoptosis depends on reactive oxygen species production, mitochondrial dysfunction, Noxa upregulation, Mcl-1 cleavage, and DNA damage. Mol. Carcinog. *52*, 118–133.

25. Khoshtinat Nikkhoi, S., Heydarzadeh, H., Ranjbar, S., Salimi, F., Aghaeifard, M., Alavian, S.M., and Reshadmanesh, A. (2016). The evaluation and comparison of transcriptionally targeted noxa and puma killer genes to initiate apoptosis under cancer-specific promoter cxcr1 in hepatocarcinoma gene therapy. Hepat. Mon. *16*, e38828.

26. Yang, X., Zhang, C., Guo, T., Feng, Y., Liu, Q., Chen, Y., and Zhang, Q. (2015). Reduced expression of microRNA-206 regulates cell proliferation via cyclinD2 in gliomas. Mol. Med. Rep. *11*, 3295–3300.

27. Malumbres, M., Sotillo, R., Santamaría, D., Galán, J., Cerezo, A., Ortega, S., Dubus, P., and Barbacid, M. (2004). Mammalian cells cycle without the D-type cyclin-dependent kinases Cdk4 and Cdk6. Cell *118*, 493–504.

28. Coqueret, O. (2003). New roles for p21 and p27 cell-cycle inhibitors: a function for each cell compartment? Trends Cell Biol. *13*, 65–70.

29. Hagenbuchner, J., Ausserlechner, M.J., Porto, V., David, R., Meister, B., Bodner, M., Villunger, A., Geiger, K., and Obexer, P. (2010). The anti-apoptotic protein BCL2L1/Bcl-xL is neutralized by pro-apoptotic PMAIP1/Noxa in neuroblastoma, thereby determining bortezomib sensitivity independent of prosurvival MCL1 expression. J. Biol. Chem. *285*, 6904–6912.

30. Knorr, K.L., Schneider, P.A., Meng, X.W., Dai, H., Smith, B.D., Hess, A.D., Karp, J.E., and Kaufmann, S.H. (2015). MLN4924 induces Noxa upregulation in acute

myelogenous leukemia and synergizes with Bcl-2 inhibitors. Cell Death Differ. *22*, 2133–2142.

31. Ishida, M., Sunamura, M., Furukawa, T., Lefter, L.P., Morita, R., Akada, M., Egawa, S., Unno, M., and Horii, A. (2008). The PMAIP1 gene on chromosome 18 is a candidate tumor suppressor gene in human pancreatic cancer. Dig. Dis. Sci. *53*, 2576–2582.

32. Wulf, G.M., Liou, Y.C., Ryo, A., Lee, S.W., and Lu, K.P. (2002). Role of Pin1 in the regulation of p53 stability and p21 transactivation, and cell cycle checkpoints in response to DNA damage. J. Biol. Chem. *277*, 47976–47979.

33. Jansson, A.K., Emterling, A.M., Arbman, G., and Sun, X.F. (2003). Noxa in colorectal cancer: a study on DNA, mRNA and protein expression. Oncogene *22*, 4675–4678.

34. Shibue, T., Suzuki, S., Okamoto, H., Yoshida, H., Ohba, Y., Takaoka, A., and Taniguchi, T. (2006). Differential contribution of Puma and Noxa in dual regulation of p53-mediated apoptotic pathways. EMBO J. *25*, 4952–4962.

35. Fujita, A., Sato, J.R., Rodrigues, L. deO., Ferreira, C.E., and Sogayar, M.C. (2006). Evaluating different methods of microarray data normalization. BMC Bioinformatics *7*, 469.

36. Wang, X., Sun, L., Wang, X., Kang, H., Ma, X., Wang, M., Lin, S., Liu, M., Dai, C., and Dai, Z. (2017). Acidified bile acids enhance tumor progression and telomerase activity of gastric cancer in mice dependent on c-Myc expression. Cancer Med. *6*, 788–797.

37. Hu, R., and Sun, X. (2016). lncRNATargets: A platform for lncRNA target prediction based on nucleic acid thermodynamics. J Bioinform Comput Biol. *14*, 1650016.